TAO, Vol. 9, No. 4, 795-812, December 1998

# Heat Flows off Southwest Taiwan: Measurements over Mud Diapirs and Estimated from Bottom Simulating Reflectors

Chuen-Tien Shyu[1], Shu-Kun Hsu[1], and Char-Shine Liu[1]

(Manuscript received 27 July 1998, in final form 30 November 1998)

## ABSTRACT

**The area offshore from southwest Taiwan is where the Taiwan mountain belt first encroaches on the Chinese continental margin. The northwestward convergence of the Luzon Arc towards the Chinese continental margin has resulted in stacking of thick sediments in terms of folds and thrusts off southwest Taiwan. Mud diapirs and bottom simulating reflectors (BSRs) are commonly observed in this region.**

**During the field experiment, the heat probe developed by the Institute of Oceanography, National Taiwan University is found to be efficient and durable. Using the newly designed heat probe, we have conducted fourteen in situ heat flow measurements off southwest Taiwan. The results show that : (1) Temperatures, temperature gradients, and thermal conductivities are anomalous and heat flows are higher above the area where mud diapirs appear. The mud diapirs are apparently influenced by relevant deep fluid migration through the pore spaces. The low heat flow found on the flank of a diapir probably results from the low thermal conductivity of mud breccia containing gas. (2) To apply the gas hydrate temperature-pressure phase diagram to derive temperature gradients from BSRs, if we speculate a gas composition of 90 percent methane and 10 percent ethane in pure water, a close estimation of the temperature gradient (only 6.3 percent less), compared with that measured in situ, is obtained.**

**(Key words: Heat probe, Heat flow, Mud diapir, BSR, Southwest Taiwan)**

## 1. INTRODUCTION

The Eurasian and Philippine Sea plates are actively interacting in the Taiwan region. Northeast of Taiwan, the Philippine Sea plate subducts beneath the Ryukyu Arc and creates the Okinawa Trough backarc basin. South of Taiwan, the lithosphere of the South China Sea subducts eastward beneath the Philippine Sea plate along the Manila Trench and creates the Luzon Arc. The northwestward convergence of the Luzon Arc acts as a pushing agent to pile

[1]Institute of Oceanography, National Taiwan University, P.O. Box 23-13, Taipei, Taiwan, ROC

up submarine sediments off southwestern Taiwan (Reed *et al.*, 1992; Liu *et al.*, 1997). The west vergent thrusts and folds of the sediments extend northward to the western foothills of Taiwan. The southwestern offshore area is indeed acting as a transition zone from rifting continental margin to compressional regime (Sibuet and Hsu, 1997). Mud diapirs have been found on the seismic profiles collected in areas with a water depth of less than 400 m along the coast (Chang, 1993; Huang, 1995) and the relevant NNE-SSW trending diapirs and anticlines are believed to extend from the near shore area to on land Taiwan (Huang, 1995; Liu *et al.*, 1997). West of the Liuchiu Hsu islet, dense anticlines mixed up with some mud diapirs and Bottom Simulating Reflectors (BSRs) are observed in some cases (Chang, 1993). BSRs are seismic reflections parallel or sub-parallel to the seafloor. They are generated by the formation of gas hydrates beneath the seafloor (Shipley *et al.*, 1979). A detailed description of BSRs distributed in the area off southwest Taiwan is given by Chi *et al.* (1998).

Sun and Liu (1993) consider that during the Pliocene mountain building of Taiwan, the anticlines were initially formed within massive mud rock and then an unbalanced loading by the thick sediments filled in extinct submarine canyons and channels on the flank, and thin sediments covered the top of the anticlines during the Pleistocene. The localized high pressure induced by the unbalanced loading plays an important role in the upward movement of mud and in initiating the mud diapirs. Chang (1993), on the other hand, suggests that during the Pliocene, the massive and thick pelagic sediment deposited in the early foreland basins in the southwestern Taiwan offshore is a source rock for diapirs and was then sealed and overlaid with neritic sediment during the Pleistocene. The overpressured mud rock may have moved upward along NE-SW trending faults, strike slip or normal, to form mud diapirs.

The outgrowing process of diapirs is , in general, associated with the rising of mud, water gas and often causes their expulsion from the seafloor through faults or conducts. The combined driving mechanisms may affect the temperature profiles on or near the mud diapirs and the heat flow values may be anomalous. Henry *et al.* (1990) detected the temperature on a large mud volcano of the Barbados accretionary complex to be close to 21°C, 19°C higher than the bottom water temperature. The heat flow on the active mound of the mud volcano is 4 times that in the surrounding basin which appears to have arisen from the action of overpressured water that comes from beneath the accretionary prism. The high heat flow is probably maintained by a continuing seepage of warm fluid through the seafloor on the active mound (Langseth *et al.*, 1988). On the other hand, heat flow values ranging between $16 \pm 5$ and $41 \pm 6$ $mWm^{-2}$ obtained from the crestal area of the Mediterranean Ridge accretionary complex, in and around the Olimpi mud diapir field are low. This suggests a rather cold conductive thermal regime, apparently not influenced by relevant upward deep fluid migration through the pore spaces while the thermal conductivity of the diapiric sediments was analyzed as ranging from 0.6 to 0.9 $Wm^{-1}K^{-1}$, which is lower than that of host hemipelagic oozes (1.15 $Wm^{-1}K^{-1}$) (Camerlenghi *et al.*, 1995). Thus, the purposes of this paper are (1) to examine the temperature and heat flow values over the mud diapir field and gas saturated areas off southwest Taiwan, (2) to correlate and discuss the results in relation to with the distribution of the diapirs, and (3) to estimate the heat flows from the BSRs and compare them with that measured in situ.

## 2. THE HEAT PROBE

Heat flow at each site is determined by independent measurements of the vertical temperature gradient and thermal conductivity in near surface sediments. Temperature gradient measurement depends on the resolution of sensors while thermal conductivity determination is quite variable and complicated. In general, in situ conductivity measurements appear to compare favorably with those made on core material aboard ship or in the laboratory (Davis *et al.*, 1984) due to disturbances caused by coring or the ambient environment (*e.g.*, pressure, temperature, water content) being different between the seafloor and the laboratory. The first in situ measurements were introduced by Sclater *et al.* (1969) but the equipment was designed to measure the conductivity of surficial sediments extending only a few centimeters beneath the sea floor. In a recent development of the in situ method with outrigged probes (Jemsek *et al.*, 1985), a line heater was located within the same probe as the thermistors used for gradient determinations. Steady heating was applied to the line heaters for a certain period (*e.g.*, 10 minutes). With continuous heating, a significant fraction of the applied heat dissipated to the sediment after the recording period was wasted. As an alternative to the steady heating method, a pulse heating method was proposed by Lister (1979). A short (*e.g.*, 10-second), calibrated heat pulse is applied to a cylindrical probe, and uses analytic approximation to fit the decay of the heat pulse to determine conductivity (Lister, 1979; Hyndman *et al.*, 1979). Von Herzon and Anderson (1972) used a solid strength member with outrigger sensors for multipenetrations and acoustic telemetry using a time interval pinger. These multipenetration and telemetry techniques have made heat flow measurements very efficient.

The heat probe used during the survey was developed at the Institute of Oceanography, National Taiwan University. It employs the 'violin bow' strength member and parallel sensor string configuration suggested by Lister (1979). It permits multiple 'pogostick' penetrations on each lowering and measures in situ thermal conductivity as well as temperature gradient over the same interval. The electronics and battery pack (normally 24 volts regulated to 16 volts) are housed in two of three high strength aluminum pressure cases which are 15 cm in diameter and 50 m in length, and are separated but connected via a pluggable bulkhead cable. In the bottom of the cases, a strength member of 3 m in length consisting of two sections (more sections for a longer probe) of a cylindrical steel rod which is 8 cm in diameter and 1.5 m in length. For additional weight, three pieces of lead, 10 cm in diameter by 30 cm in length are attached to the space between cases. The total weight of the equipment is about 300 kg. A relatively slim sensor tube of 4 mm in diameter and 3 m in length is attached at the base of the pressure case containing the electronics and is supported by three 8 cm-high fins attached to the rod. For use in rough conditions and the absorption of impulsive force, both ends of the tube have been strengthened with brass clamps. The internal material of the tube contains : 7 pairs of teflon insulated thermistor lead wires, 7 thermistors of 40 cm distributed at equal intervals, mineral oil filling, and a pair of vanish-insulated heater wires. The effective delay time, where the tube reaches its maximum temperature in a significant time after onset of the heat pulse generated by the heater wire, is about 35 ~ 40 seconds.

The automatic control and recording system provide a 7-channel 16-bit digital resolution, and the entire data can be stored in 128 K bytes of battery backed up RAM for about 10

hours' continuous recording at a 5 sec sampling rate. Meticulous mechanical and electronic design has resulted in attaining temperature resolution of 0.0004°C in the range of -1 to 25 °C. To properly trigger the heat pulse after probe penetration, a tilt sensor module ranging 0 to 60 degrees from vertical is installed. The variation and stability information from the tilt sensor can indicate the correct impact time of the probe with the seafloor and the time when it is pulled out by the wire. The recording system is designed to be operated via personal computers. Data transfer and system checks can be run without opening the pressure cases.

## 3. FIELD MEASUREMENTS

The data presented in this paper were collected aboard the R/V Ocean Researcher I in November 1996. Navigation was done using the Global Positioning System (GPS). Heat flows were determined from temperature measurements with the thermistor sensors equally spaced inside a steel tube. The thermal conductivities were measured using the pulse heating method (Lister, 1979).

During the heat flow measurement, the research vessel sails to the sites selected in the survey area (Figure 1), stops drifting, and lowers the probe to a depth of about 30 m above the seafloor for about 5 minutes. During that period, the wire and probe will swing back to an equilibrium position almost perpendicular to the seafloor, and the "zero-gradient" reference temperatures are recorded for later data correction. Then, the probe with a heavy weight of about 300 kg on top of it falls freely to and penetrates the bottom. After penetration, wire must be run out continuously as the ship moves on. The difficulty in maintaining the ship directly over the instrument in the bottom during this period is overcome by the GPS navigation which provides continuous positioning information during the survey with an accuracy of about $\pm 25$ m. During each penetration, the instrument remains undisturbed in the bottom for about 23 minutes to measure temperature and in situ thermal conductivity (8 minutes for the temperature gradient; 15 minutes for the thermal conductivity). Although the heat probe has the capability of multipenetration, due to the constraint of the cruise time, only one penetration was attempted at each site in this study. The heat flow measurement sites are relatively subdued to the adjacent sediment bottom chosen mainly along the previous seismic survey profiles off southwestern Taiwan (Figure 1). No basement outcrops were detected at any of the sites.

## 4. DATA REDUCTION

A temperature-time record of a typical penetration is shown in Figure 2; for simplicity, data from only two of the seven thermistors are shown. The record indicates clearly (1) the time period prior to final descent and penetration, during which constant depth and temperature of the tube are maintained, (2) the thermal decay following a slight temperature rise which resulted from the impact of the probe with the sediments (impact decay), and (3) the thermal decay following the calibrated heat pulse (heat pulse decay). The temperature gradients are calculated from the data during the impact decay period (about 8 minutes). Relative temperature-depth data and their uncertainties are determined and corrected by extrapolation of the impact heating decay at each thermistor, and from the relative temperature measured after penetration with the probe hanging stationary in the isothermal near-bottom water prior to

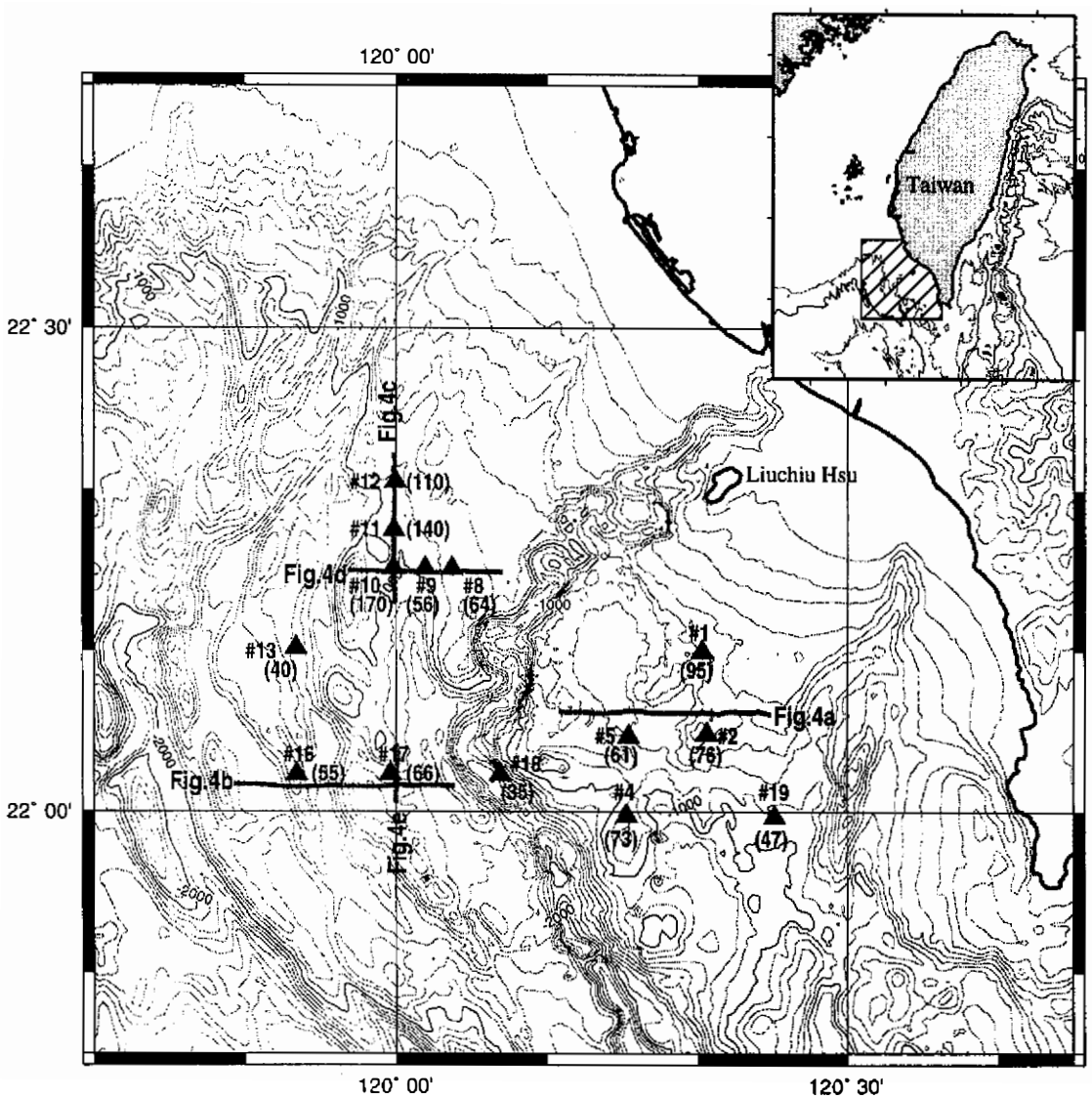


*Fig. 1.* Locations (▲) of heat flow sites (#) and seismic tracks (▬) in the southwestern Taiwan offshore. Parenthetical values are heat flows in mW/m². Seismic profiles are shown in Figure 4.

penetration. The temperature extrapolated according to the cylindrical decay function $F(\alpha, \tau)$ (Bullard, 1954) from the impact (origin) time is least squares fitted to the data by successively adjusting the thermal conductivity K (and therefore the diffusivity) and the origin time. The corrected and extrapolated temperatures for the thermistors are used to calculate gradients for

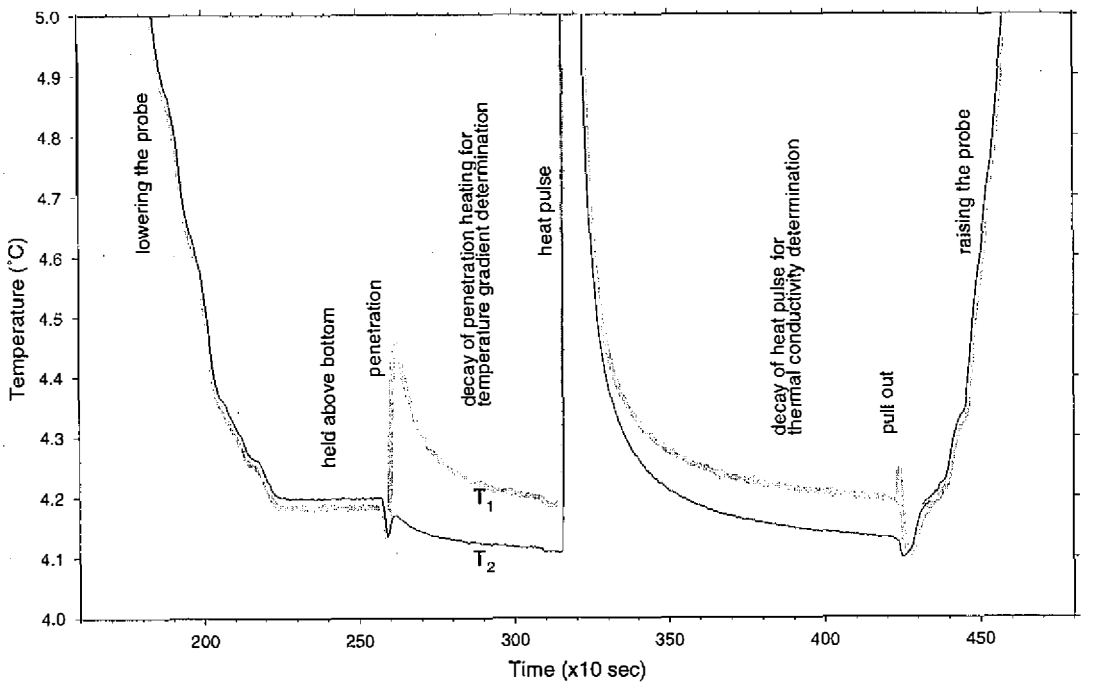


*Fig. 2.* An example of temperature vs. time during heat flow measuring process (only 2 of 7 thermistors' response are shown).

each section. In situ thermal conductivity is calculated from about 15 minutes of recording which immediately follows the start of a heat pulse. Theoretically, if a perfectly conducting cylindrical tube is inserted into a material with initial temperature $T_0$, the temperature at a time t is given by (Bullard, 1954; Jaeger, 1956; Carslaw and Jaeger, 1959):

$$T = T_0 F(\alpha, \tau)$$

where

$$F(\alpha,\tau) = \frac{4\alpha}{\pi^2}\int_0^{\alpha} \frac{\exp(-\tau u^2)du}{u\Delta(u)}$$

and

$$\Delta(u) = [uJ_0(u) - \alpha J_1(u)]^2 + [uY_0(u) - \alpha Y_1(u)]^2$$

$J_n(u)$ and $Y_n(u)$ are Bessel funcitons of order n of the first and second kinds, $\tau = \kappa\ t/a^2$ is the time constant of the probe of radius a in material of diffusivity $\kappa$, and $\alpha = 2\pi a^2 \rho c / S$ is twice the ratio of the heat capacity of the material to that of the probe. $\rho$ and $c$ are the density and specific heat of the material, respectively. $S$ is the heat capacity of the probe. Intuitively,

the solution can be least squares fitted to the data by the continuous selection of origin time, conductivity and diffusivity similar to that in obtaining temperature gradients. The main difference is that the heating pulse is calibrated and may raise the temperature to as high as 8 °C above that of sediment, while the impact heat is variable and in general less than 0.5 °C. In order to avoid the influence of impact heat, a delay of about 8 minutes is recommended for temperature gradient determination from the thermal decay curve after the initial impact, and a delay of about 15 minutes after the generation of the heat pulse is recommended for conductivity calculation. It is interesting and important property that the temperature solution is dominated by the conductivity K; for $\tau>1$ and $\alpha=2$ the solution reduces to the asymptotic solution $t \approx T_0 / 2\alpha\tau$ (Blackwell, 1954; Lister, 1979; Hyndman *et al.*, 1979). Except in sediments of highly unusual properties, the heat capacities need not be estimated and $\alpha=2$ is applicable to most cases (Lister, 1979). The steel thermal probes used during the survey are 0.8 cm in diameter and are filled with mineral oil along with thermistor lead wires, heating wires, and fibre braid wrapped around the wires and the heat capacities, $S$, of the probes are 187.72 (Joul/m°C). For $\tau>10$ the error asymptotic approach is less than 5.5% of the time solution. We consider it adequate to fit the asymptotic solution to the data if K is greater than 0.8 $Wm^{-1} K^{-1}$. This means the probe must stay in the bottom for more than 12 minutes after the heat pulse is triggered (more time is needed if K is less than 0.8 $Wm^{-1} K^{-1}$, *e.g.* about 18 minutes is needed for K=0.6 $Wm^{-1} K^{-1}$).

### 4.1 Temperature Gradients

The temperature gradients measured are given in Figure 3. In general, they show little, if any, departure from linearity. Together with the bottom water temperature, these gradients were also used to determine the depth penetration. Average gradient values are determined from the best unweighted linear fit of equilibrium temperatures versus depth. Note that there are a few sites (*e.g.*, Sites 1,4,10,11,12; see Table 1) where the temperature gradients are significantly higher than those of the other sites. It is noted that stations 10,11 and 12 are located near mud diapirs (Figures 1 and 4 (c)) and Sites 1 and 4 are on top of a fault and an anticline, respectively. These high temperature gradients should be analyzed together with thermal conductivities to reveal their true thermal characteristics.

### 4.2 Thermal Conductivities

The thermal conductivity data at each site (Table 1 and Figure 3) are reasonably well constrained. Their variations with respect to the mean value are less than 10%, except that of Site 4 which is about 18% lower than the mean and may reflect lateral variation in sediment types or physical properties. Sediments at Site 4 are of mudstone and brecciated mudstone deposits transported by Kaoping canyon turbidities. The average grain size fraction, $\phi$, of the sticky mud is 7.41 (or diameter=5.88 $\mu$m) (Chern, 1997), which is considerably smaller (by 26%) than the mean grain size at the other sites. The thermal conductivity of the seafloor is highly dependent upon the proportion of water contained in the sediments and is generally proportional to the fractional content of water by mass (Ratcliffe, 1960; Bullard and Day,

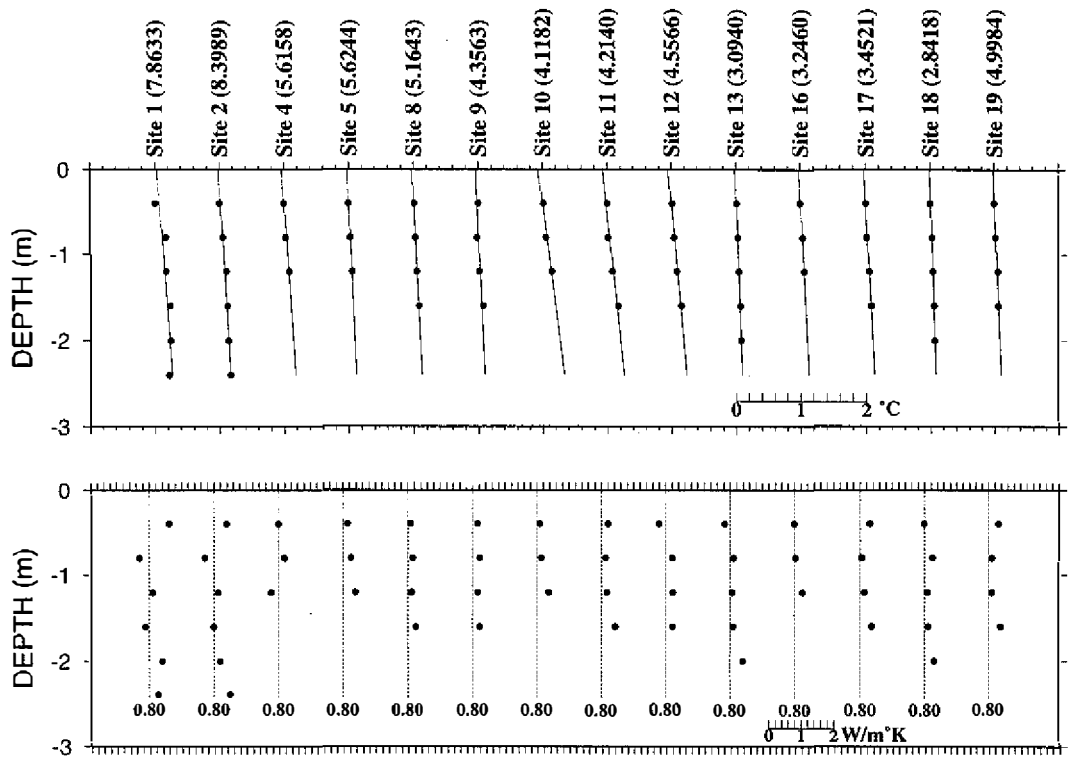


*Fig. 3.* Temperature (upper box) and thermal conductivity (lower box) profiles for each site. Origin of depth axis is position of ocean floor.

1961; Lachenbruch and Marshall, 1966). The smaller grain size and sticky properties may significantly reduce the water content and therefore the conductivity of the sediments at Site 4. For the other 13 sites, the conductivities are generally uniform with a mean value of $0.97 \pm 0.07$ $Wm^{-1}$ $K^{-1}$ which is similar to or slightly higher than that of typical marine sediments. For a given depth interval, conductivities generally vary inversely with temperature gradients, as would be expected for uniform heat flow over a site. Although there are some differences in mean conductivities between sites, systematic increase with depth is obvious at most of the sites, with the exception of Sites 1,4,9 and 12, to the maximum depth of probe penetration.

## 5. HEAT FLOWS ON MUD DIAPIRS

Figure 1 shows the heat flow measurement locations and their corresponding single-channel seismic lines as used for the interpretation. Excluding the tectonically active zone, the average heat flow for the ocean basin is about 62 $mW/m^2$. High heat flows of 72, 66 and 110 $mW/m^2$ occur on the summit or in the vicinity of the mud diapirs (Figures 4(a), 4(b), and 4(c), respectively) indicating recent mud extrusion activities and continuing seepage of mud and

Table 1. Heat flow results in the southwest offshore area of Taiwan.

| Site | Latitude N | Longitude E | WD m | K W/m°K | G °K/m | Q mW/m$^2$ | Relevant Structure |
|---|---|---|---|---|---|---|---|
| 1 | 22.1658 | 120.3385 | 552 | 0.963 | 0.099 | 95 | fault |
| 2 | 22.0800 | 120.3438 | 545 | 0.952 | 0.080 | 76 | diapir |
| 4 | 21.9952 | 120.2548 | 783 | 0.787 | 0.093 | 73 | anticline |
| 5 | 22.0778 | 120.2567 | 835 | 1.057 | 0.058 | 61 | |
| 8 | 22.2520 | 120.0615 | 840 | 0.955 | 0.067 | 64 | BSR |
| 9 | 22.2522 | 120.0320 | 956 | 0.980 | 0.057 | 56 | BSR |
| 10 | 22.2523 | 119.9968 | 964 | 0.993 | 0.171 | 170 | anticline, diapir |
| 11 | 22.2918 | 119.9975 | 953 | 1.030 | 0.136 | 140 | anticline, diapir |
| 12 | 22.3413 | 119.9990 | 907 | 0.905 | 0.122 | 110 | diapir ? |
| 13 | 22.1700 | 119.8897 | 1413 | 0.894 | 0.045 | 40 | depression |
| 16 | 22.0387 | 119.8905 | 1285 | 0.887 | 0.062 | 55 | diapir |
| 17 | 22.0392 | 119.9937 | 1219 | 1.013 | 0.065 | 66 | BSR |
| 18 | 22.0390 | 120.1147 | 1545 | 0.940 | 0.037 | 35 | canyon |
| 19 | 21.9942 | 120.4192 | 909 | 1.025 | 0.046 | 47 | |

WD= water depth, K= thermal conductivity, G= temperature gradient, Q= heat flow.

water through the seafloor. All the temperature profiles on or near the mud diapirs indicate that the temperature gradients are high and uniform with depth, which implies that the vertical flux of interstitial fluid is less than about 10 cm/yr (Langseth *et al.*, 1988). Heat flow values over diapiric anticlines are anomalously high (Figure 4(c)), the highest value being 170 mW/m$^2$ which is nearly three times the basin value. It can be noted that the heat flow values increase southward to the diapiric anticline. However, a relatively low value (55 mW/m$^2$) was found on the flank of the diapir (Figure 4(b)) which results from the presence of low thermal conductivity (Table 1). This could be explained by assuming that the mud breccia contains gas. In general, the positive heat flow anomalies over the mud diapirs off the southwestern Taiwan is consistent with those reported by Langseth *et al.* (1988), who observed a peak heat flow value of 200 mW/m$^2$ at a mud volcano seaward of the Barbados Ridge Complex. Our results are, however, contrary to those of Camerlenghi *et al.* (1996). They have obtained low heat flow values from the crestal area of a ridge in and around the Olimpi mud diapir field, and have suggested a rather cold conductive thermal regime, apparently not influenced by relevant upward deep fluid migration through the pore spaces.

## 6. ESTIMATES OF HEAT FLOW FROM GAS HYDRATES

Bottom simulating reflectors (BSRs) are often observed in marine seismic reflection data from continental slopes and rises, many of which are associated with the accretionary prism

and imbricate wedge (Katz, 1982; Lewis and Pettinga, 1993). Geometric relations, reflection coefficients, reflection polarity and pressure-temperature relations all support the anomalous reflectors are the base of gas hydrated sediments (Markl *et al.*, 1970: Bryan, 1974: DSDP Leg 76 Scientific Party, 1981). In sediments containing sufficient amounts of gases such as methane, ethane, and carbon dioxide, the gas may combine with water to form gas hydrates, which are crystalline icelike substances (Bryan, 1974). These substances may be formed under appropriate pressure and temperature conditions when water is saturated with gas (Stoll *et al.*, 1971; Claypool and Kaplan, 1974; Miller, 1974; Shipley *et al.*, 1979; Macleod, 1982; Minshull and White, 1989). The in situ temperature at a BSR can be estimated when the pressure and gas composition are known. The pressure at a BSR is calculated on the basis of its depth below the seabed, from which the corresponding temperature is obtained using the gas hydrate temperature-pressure phase diagram (Figure 5). Shipley *et al.* (1979) estimated thermal gradients from the depth of the BSR boundaries on continental slopes and rises; Yamano *et al.* (1982) estimated heat-flow values in the Nankai Trough around Central America, and along the Blake Outer Ridge through additional inferred thermal conductivity of sediments. Townend (1997) concluded that BSR data are very useful in determining offshore heat flow around New Zealand, and suggested that heat flow estimates need to be corrected for the thermal effects of ongoing sediment deposition. In the following, we derive the temperature gradients from the estimated pressure at the depths of BSRs and compare them with those measured in situ, and speculate

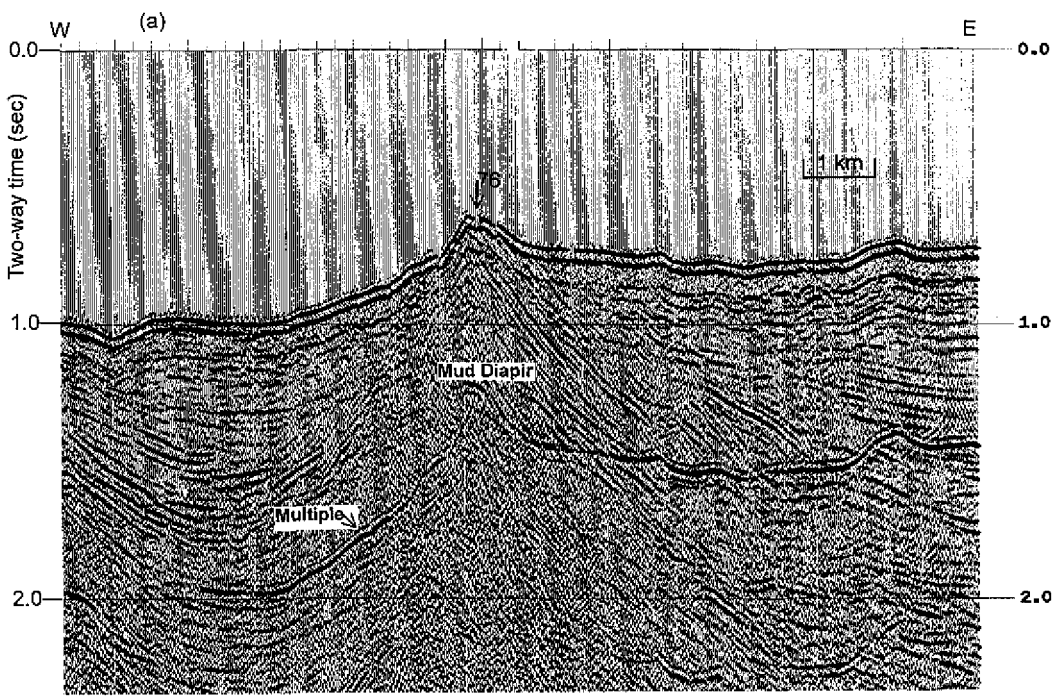


*Fig. 4.* Heat flow sites and corresponding seismic profiles. Heat flows are in $mW/m^2$.

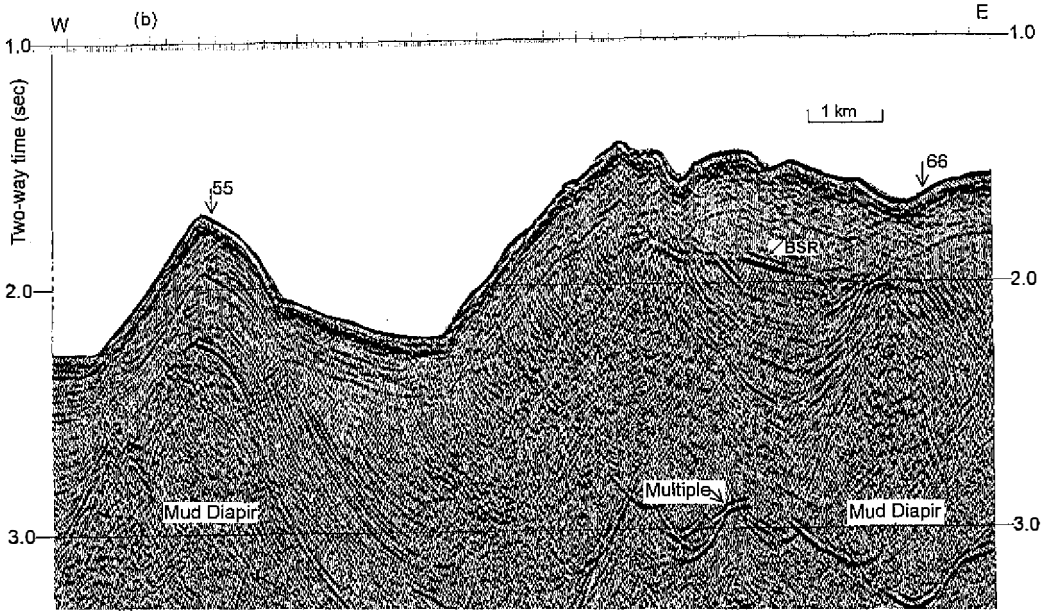


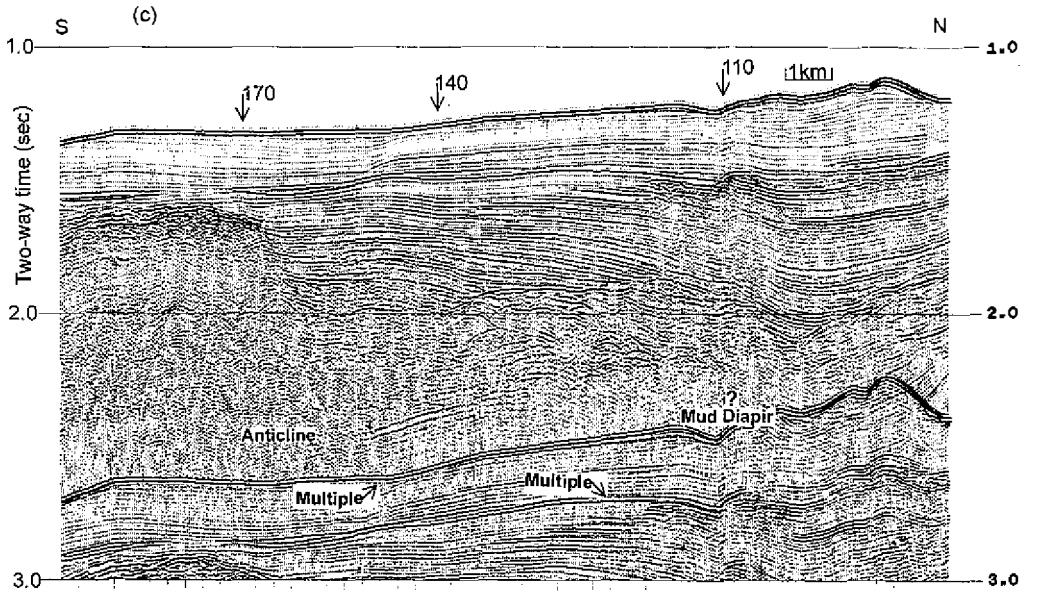


(*Fig. 4.* continued)

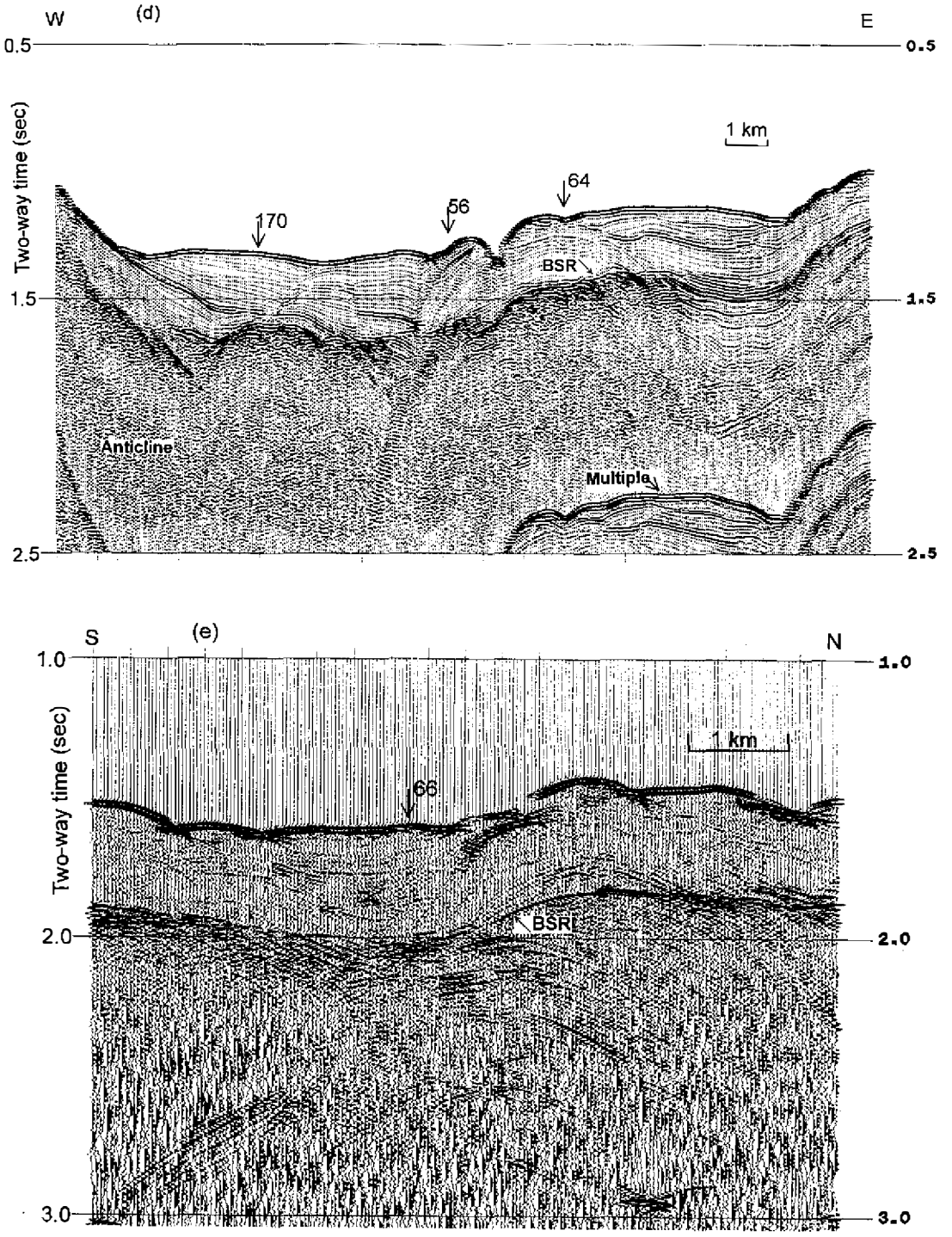


(*Fig. 4*. continued)

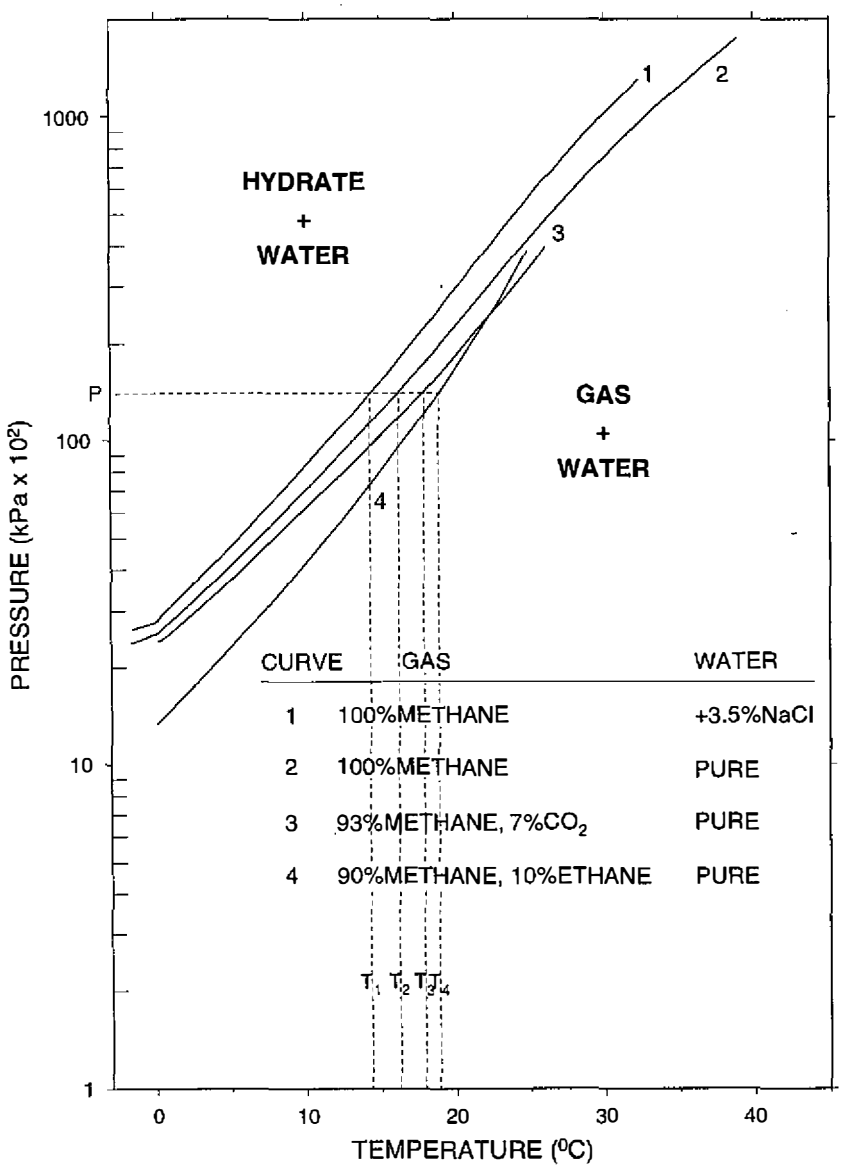


*Fig. 5.* Pressure and temperature stability conditions for gas hydrates. For example, we may draw a horizontal dotted line from P (a given pressure) to meet curves 1, 2, 3, and 4 and from these crossing points draw vertical dotted lines to meet temperature axis at $T_1$, $T_2$, $T_3$ and $T_4$. Highest temperature $T_4$ derived from curve 4 gives a reasonable temperature gradient compared with that measured in southwestern Taiwan area. Gas hydrate stability relations are adapted from Macleod (1982) and Minshull and White (1989).

the possible composition of BSRs. The method used here is basically similar to that initially proposed by Yamano *et al.* (1982) and discussed in detail by Minshull and White (1989).

Those heat flow sites located above BSRs on the seismic sections are certainly good examples for verifying the method. Figures 4(d) and 4(e) show the E-W and N-S seismic profiles across heat flow sites to be 64, 56, 170 and 66 mW/m$^2$, respectively. The seafloor temperature is determined during the heat flow measurements at the surface of the sediments. Seismic interval velocities, and itheir relation with density (Hamilton, 1978) are used to calculate BSR depths and pressure. BSR temperatures are thereby estimated using an interpolation of the appropriate gas hydrate stability curve (MacLeod, 1982; Minshull and White, 1989; Townend, 1997). Since there is no core measurement available, the density estimated from the sound velocity is not unique, and the control of the gas and water composition is poor. These two parameters have to be determined through trial and error by substituting them into the hydrate stability curve. Assuming a constant temperature gradient, in general, increasing the density by 10% would give only a negligible 1~2% increase in the gradient. However, if 90% methane + 10% ethane was assumed as the condition (curve 4, Figure 5), instead of 93% methane + 7% CO2 (curve3, Figure 5), the predicted temperature gradients would increase from 3.5% to as much as 12.6%. The deeper the BSR, the larger the increase. If the other two curves (curves 1 and 2) of different phases are used, they may give values for temperature gradients lower by 11%~41.7% compared with those obtained from curve 3. Owing to the fact that the measured temperature gradients of about 63 °C/1000 m on average (excluding the anomalous high value at Site 10), on top of BSRs are higher than those derived through curves 1, 2 and 3, it is reasoned that curve 4 of the methane hydrate stability curve has a closer relationship to the data (dotted lines, Figure 5). That is , the BSRs in this area are most likely to consist of 90% methane, 10% ethane and pure water. The base of the gas hydrate is strongly affected by changes in geothermal gradients associated with diapirs. Even though the average temperature gradient derived from the BSRs is 0.059 °C/m, which is less than that measured (0.063 °C/m) by 6.3% (Table 2), it is considered to have a good consistency comparing with that of the others (Yamano *et al.*, 1982; Townend, 1997). Parameters such as seismic velocity,

Table 2. Temperature gradients derived from BSR.

| Site | $W_D$ m | $T_f$ ℃ | $\rho_s$ g cm$^{-3}$ | $V_p$ m sec$^{-1}$ | $D_{BSR}$ m | $G_{BSR}$ °Km$^{-1}$ | $G_M$ °Km$^{-1}$ |
|---|---|---|---|---|---|---|---|
| 8 | 840 | 5.164 | 1.64 | 1610 | 208 | 0.061 | 0.067 |
| 9 | 956 | 4.356 | 1.65 | 1620 | 228 | 0.063 | 0.057 |
| 10 | 964 | 4.118 | 1.63 | 1600 | 181 | 0.078 | 0.171 |
| 17 | 1219 | 3.452 | 1.68 | 1650 | 325 | 0.052 | 0.065 |

$W_D$ = water depth, $T_f$ =temperature of seabed, $\rho_s$ = average density from seabed to BSR, $V_p$ = average seismic velocity, $D_{BSR}$ = depth of BSR below the seabed, $G_{BSR}$ = temperature gra

gas composition, thickness of BSRs and sedimentation rate are the primary error sources for the temperature estimation. Moreover, since the data from only three sites are available for the comparison, the consistency between the estimation from BSRs and that from conventional measurements in this experiment still need further investigation.

## 7. CONCLUSIONS

We strengthened the ends of the sensor tube with brass clamps to absorb the impact force during heat probe penetration and found that this may significantly increase the durability in rough operating conditions. By utilizing the variation and stability information of a tilt sensor instead of a motion sensor, the heat probe is able to follow the desired process correctly to measure the in situ temperature gradient and conductivity. This modification has allowed precise execution of automated commands during the field experiment and has also reduced the cost of heat probe .

Fourteen heat flow sites located offshore from southwestern Taiwan are surveyed. In general, the measured temperature gradients show little, if any, departure from linearity. A few sites are located near mud diapirs, faults, and anticlines. The temperature gradients of these sites are significantly higher than the others. Except for Site 4 (located above an anticline), the mean conductivites generally vary inversely with temperature gradients, as would be expected for uniform heat flow over sites.

The high heat flow group, such as 76, 66, 110, and 170 $mW/m^2$, occur on the summit or in the vicinity of mud diapirs and indicate recent occurrence of mud and water seepage through the seafloor. A relatively low heat flow (55 $mW/m^2$) found on the flank of a diapir results from the presence of low thermal conductivity that could be explained by assuming that the mud breccia contains gas. In general, the positive heat flow anomalies over the mud diapir field off southwestern Taiwan are consistent with those reported by Langseth *et al.* (1988) but contrary to those found by Camerlenghi *et al.* (1996). For further study of the subject, denser measurements across mud diapirs are highly necessary.

Three heat flow sites over the BSRs have been verified for estimating temperature gradients. Our results imply that the BSRs in this area mainly consist of 90% methane, 10% ethane and pure water. The average temperature gradient derived from BSRs is 0.059 °C/m, which is about 6.3% less than that measured, but is still considered to have a good consistency compared with results from other studies (Yamano *et al.*, 1982; Townend, 1997). However, analyses are based on data from only three sites, so further investigation is desirable.

**Acknowledgments** The authors thank the officers, crew, and shipboard technicians of the R/V Ocean Researcher I and Mr. S.D. Chiou of the Ocean Research Vessels Instrument Center for the heat flow data acquisition. C.W. Wang and S.Y. Liu deserve special thanks for their help in editing and processing the heat flow and seismic reflection data. We acknowledge the efforts of electronic engineer H.I. Chang in the construction of the recording system of the instrument. The study was supported by the National Science Council of the Republic of China, under grants NSC85-2611-M-002A-004 and NSC86-2117-M-002A-002-ODP.

## REFERENCES

Blackwell, J. H., 1954: A transient flow method for determination of thermal constraints of insulating materials in bulk. *J. Appl. Phys.*, **25**, 137-144.

Bryan, G. M., 1974: In situ indications of gas hydrate, in Natural gases in marine sediments. *Mar. Sci.*, **3**, 299-308.

Bullard, E. C., 1954: The flow of heat through the floor of the Atlantic Ocean. Proc R. Soc. London A, 222, 408-429.

Bullard, E. C., and A. A. Day, 1961: The flow of heat through the floor of theAtlantic Ocean. *Geophys. J.*, **4**, 282-292.

Camerlenghi, A., M. B. Cita, B. Della Vedova, N. Fusi, L. Mirabile, and G. Pellis, 1995: Geophysical evidence of mud diapirism on the Mediterranean Ridge Accretionary Complex. *Mar. Geophys. Res.*, **17**, 115-141.

Carslaw, H. S., and J. C. Jaeger, 1959: Conduction of heat in solids, 2nd edn., Oxford University Press, London, 510pp.

Chang, C. H., 1993: The study of the mud diapirs offshore from southwestern Taiwan (in Chinese). M. Sc. thesis, Inst. Oceanogr., Natl. Taiwan Univ., Taipei, 63pp.

Chern, Y. C., 1997: Sedimentology of surface sediments off southwest Taiwan (in Chinese), Ph. D. dissertation, Inst. Oceanogr., Natl. Taiwan Univ., Taipei, 160pp.

Chi, W. C., D. L. Reed, C. S. Liu, and N. Lundberg, 1998: Distribution of the bottom-simulating reflector in the offshore Taiwan collision zone. *TAO,* **9**, 779-794.

Claypool, G. W., and I. R. Kaplan, 1974: The origin and distribution of methane in marine sediments, in natural gases in marine sediments. *Mar. Sci.*, **3**, 99-139.

Davis, E. E., C. R. B. Lister, and J. G. Sclator, 1984: Toward determining the thermal state of old ocean lithosphere: Heat flow measurements from the Blake-Bahama outer ridge, N. W. Atlantic. *Geoph. J. R. Astr. Soc.*, **78**, 507-545.

DSDP Leg 76 Scientific Party, 1981: Challenger drills at sites off east coast, Geotimes, 26:23-25.

Hamilton, E. L., 1978: Variations of density and porosity with depth in deep-sea sediments. *J. Sediment. Petrol.*, **46**, 280-300.

Henry, P., X. Le Pichon, S. Lallemant, J. Foucher, G. Weatbrook, and M. Hobart, 1990: Mud volcano field seaward of the Barbados Accretionary Complex: A deep-towed side scan sonar survey. *J. Geophys. Res.*, **95**, 8917-8929.

Huang, W. L., 1995: Distribution of the mud diapirs offshore from southwestern Taiwan, their relationships to the onland anticlinal structures and their effects on the deposition enviroment in southwestern Taiwan (in Chinese). M. Sc. thesis, Inst. Oceanogr., Natl. Taiwan Univ., Taipei, 68pp.

Hyndman, R. D., E. E. Davis, and J. A. Wright, 1979: The measurement of marine geothermal heat flow by a multipenetration probe with digital acoustic telemetry and in situ thermal conductivity. *Mar. Geophys. Res.*, **4**, 181-205.

Jaeger, J. C., 1956: Conduction of heat in an infinite region bounded internally by a circular cylinder of a perfect conductor. *Australian J. Physics*, **9**, 167-179.

Jemsek, J., R. Von Herzen, and P. Andrew, 1985: In-situ measurement of thermal conductivity using the continuous-heating line source method and WHOI outrigged probe, Tech. Report WHOI-85-28, Woods Hole Oceanographic Institution, 73pp.

Katz, H. R., 1982: Evidence for gas hydrates beneath the continental slope, East coast, North Island, New Zealand, N. Z.. *J. Geol. Geophys.*, *25*, 193-199.

Lachenbruch, A. H., and B. V. Marshall, 1966: Heat flow through the Arctic Ocean floor: the Canada Basin-Alpha Rise boundary. *J. Geophys. Res.*, **71**, 1223-1248.

Langseth, M. G., G. K. Wesbrook, and M. A. Hobart, 1988: Geophysical survey of a mud volcano seaward of the Barbados Ridge Accretionary Complex. *J. Geophys. Res.*, **93**, 1049-1061.

Lewis, K. B., and J. A. Pettinga, 1993: The emerging imbricate frontal wedge of the Hikurangi margin. South Pacific Sedimentary Basins , Elsevier. In : P. F. Balance (Ed.), Amsterdam, 225-250.

Lister, C. R. B., 1979: The pulse-probe method of conductivity measurement. *Geophys. J. R. Astron. Soc.*, **57**, 451-461.

Liu, C. S., I. L. Huang, and L. S. Teng. 1997: Structural features off southwestern Taiwan. *Mar. Geol.*, **137**, 305-319.

Macleod, M. K., 1982: Gas hydrates in ocean bottom sediments. *AAPG Bull*, **66**, 2649-2662.

Markl, R. G., G. M. Bryan, and J. I. Ewing, 1970: Structure of the Blake-Bahama Outer Ridge. *J. Geophys. Res.*, **75**, 4539-4555.

Miller, S. L., 1974: The Nature and occurrence of clathrate hydrates, in: Natural Gases in marine sediments. *Mar. Sci.*, **3**, 151-177.

Minshull T., and R. White, 1989: Sediment compaction and fluid migration in the Makran accretionary prism. *J. Geophys. Res.*, **94**, 7387-7402.

Ratcliff, E. H. 1960: The thermal conductivities of ocean sediments. *J. Geophys. Res.*, **65**, 1535-1541.

Reed, D. L., N. Lundberg, C. S. Liu, and B. Y. Kuo, 1992: Structural relations along the margins of the offshore Taiwan accretionary wedge: implications for accretion and crustral kinematics. *Acta Geol. Taiwanica*, **30**, 105-122.

Sclater, J. G., C. E. Corry, and V. Vacquier, 1969: In-situ measurement of the thermal conductivity of ocean floor sediments. *J. Geoph. Res.*, **74**, 1070-1081.

Shipley, T. H., M. H. Houston, R. T. Buffler, F. J. Shaub, K. J. Mcmillen, J. WLadd, and J. L. Worzel, 1979: Seismic evidence for widespread possible gas hydrate horizons on continental slopes and rises. *AAPG Bull*, **63**, 2204-2213.

Sibuet, J. C., and S. K. Hsu, 1977: Geodynamics of the Taiwan arc-arc collision. *Tectonophysics*, **274**, 221-251.

Stoll, R. D., J. Ewing, and G. M. Bryan, 1971: Anomalous wave velocities in sediments containing gas hydrates. *J. Geophys. Res.*, **76**, 2090-2094.

Sun, S. C., and C. S. Liu, 1993: Mud diapirs and submarine channel deposits in offshore Kaohsiung-Hengchun, southwest Taiwan. *Pet. Geol. Taiwan*, **28**, 1-14.

Townend, J., 1997: Estimates of conductive heat flow through bottom-simulating reflectors on the Hikurangi and southwest Fiordland continental margins, New Zealand. *Mar.*

*Geol.*, **141**, 209-220.

Von Herzen, R. P., and R. N. Anderson, 1972: Implications of heat flow and bottom water temperature in the eastern equatorial Pacific. *Geeophys. J.*, **26**, 427-458.

Yamano, M., S. Uyeda, Y. Aoki, and T. H. Shipley, 1982: Estimates of heat flow derived from gas hydrates. *Geology*, **10**, 339-343.